PHYSICAL REVIEW B **70**, 245114 (2004)

de Haas–van Alphen and chemical potential oscillations in the magnetic-breakdown quasi-two-dimensional organic conductor κ-(BEDT-TTF)$_2$Cu(NCS)$_2$

V. M. Gvozdikov*
Max-Planck-Institut für Physik komplexer Systeme, Nöthnitzer Strasse 38, D-01187 Dresden, Germany

A. G. M. Jansen
Service de Physique Statistique, Magnétisme, et Supraconductivité, Département de Recherche Fondamentale sur la Matière Condensée, CEA-Grenoble, 38054 Grenoble Cedex 9, France

D. A. Pesin
Department of Physics, University of Washington, Box 351560, Seattle, Washington 98165-1560, USA

I. D. Vagner
Grenoble High Magnetic Field Laboratory, Max-Planck-Institut für Festköperforschung and Centre National de la Recherche Scientifique, F-38042 Grenoble, Cedex 9, France

P. Wyder
Grenoble High Magnetic Field Laboratory, Max-Planck -Institute für Festköperforshung and Centre National de la Recherche Scientifique, F-38042 Grenoble, Cedex 9, France

(Received 8 April 2004; revised manuscript received 19 August 2004; published 15 December 2004)

We present an analytical theory for the de Haas–van Alphen (dHvA) oscillations in layered organic conductors such as κ-(BEDT-TTF)$_2$Cu(NCS)$_2$ which takes into account the magnetic breakdown and the chemical potential oscillations. For this purpose we have generalized our theory for the chemical potential oscillations in layered conductors [V.M. Gvozdikov, A.G.M. Jansen, D.I. Pesin, I.D. Vagner, and P. Wyder, Phys. Rev. B **68**, 155107 (2003)] to the case of an arbitrary electron dispersion within the layers. Such an approach gives a better agreement with an experimental data for κ-(BEDT-TTF)$_2$Cu(NCS)$_2$ salt than that taking account of the magnetic breakdown (MB) only [V.M. Gvozdikov, Yu.V. Pershin, E. Steep, A.G.M. Jansen, and P. Wyder, Phys. Rev. B **65**, 165102 (2002)]. The magnetization oscillation patterns and the peaks in the fast Fourier transforms (FFT's) are studied in different combinations of the stochastic and coherent MB regimes with and without the chemical potential oscillations. It is shown that that the chemical potential oscillations in the coherent and stochastic MB regimes do not affect the α and β peaks, but change the amplitudes of the higher harmonics and satellites around the β peak. In the FFT spectrum of κ-(BEDT-TTF)$_2$Cu(NCS)$_2$ two satellites are resolved: $\beta-\alpha$ (the so called "forbidden" peak) and $\beta+\alpha$. In the stochastic MB regime all satellites are depressed. In the coherent MB regime with fixed chemical potential they are higher and have equal amplitudes. Only in the coherent MB regime with oscillating chemical potential the "forbidden" peak $\beta-\alpha$ becomes larger than the satellite $\beta+\alpha$ and the calculated FFT spectrum conforms with the FFT spectrum of the dHvA signal of κ-(BEDT-TTF)$_2$Cu(NCS)$_2$.

DOI: 10.1103/PhysRevB.70.245114 PACS number(s): 71.18.+y, 75.20.En, 73.50.Jt, 74.70.Kn

I. INTRODUCTION

The experimental observation of the quantum oscillations of the magnetization and conductivity based on the Lifshitz-Kosevich (LK) theory[1] proved to be one of the most powerful tools for Fermi-surface studies in conventional metals.[2,3] This approach as well gives an experimental information about the values of effective electron masses, scattering times, gyromagnetic factors for different cross sections of the Fermi surfaces of conventional metals. On the other hand, a direct application of the LK theory to the new organic conductors runs against some difficulties caused by the fact that this theory does not take into account some important features of the quasi-two-dimensional (Q2D) conductors. Among these, in particular, are the chemical potential oscillations[4–10] and magnetic breakdown.[11] The de Haas–van Alphen (dHvA)[12–14] and Shubnikov–de Haas (SdH)[15–20] studies of the layered organic Q2D conductors based on the molecule BEDT-TTF, also known as ET salts (see Ref. 21) have shown numerous deviations from the standard LK theory.[1]

In 3D conductors the chemical potential is fixed at the Fermi level ε_F because electrons populating the parabolic Landau bands below ε_F stabilize its position. This is in a sharp contrast to the 2D case, where the Landau levels are flat and the chemical potential at zero temperature jumps between the two upper populated levels with the amplitude $\hbar\omega_c$. In the 3D case, the amplitude of the chemical potential oscillation is strongly reduced to the value $\hbar\omega_c\sqrt{\hbar\omega_c/\varepsilon_F}$, which is much smaller than $\hbar\omega_c$ since $\hbar\omega_c \ll \varepsilon_F$. In the layered organic conductors and superlattices the Landau energy spectrum is neither flat nor parabolic because energy bands evolve due to the interlayer electron hopping. The chemical potential oscillations for this case was studied in our paper[10] under the assumption that within the layers electrons behave as a free gas. This is not true for the organic layered conductors, such as the ET salts,[21] which have a complex 2D Fermi surface within the planes. The generalization of this result to the case of an arbitrary dispersion of electrons in the layers is one of the purposes of the present paper. We then apply the theory of the chemical potential oscillations to the layered organic ET salt κ-(BEDT-TTF)$_2$Cu(NCS)$_2$. The 2D Fermi surface of this conductor consists of the two open sheets with closed orbits in between and implies a magnetic breakdown. Another aim is to calculate the dHvA oscillations for Q2D metals, like such as κ-(BEDT-TTF)$_2$Cu(NCS)$_2$, taking into account both the magnetic breakdown and chemical potential oscillations.

The magnetic breakdown (MB) in κ-(BEDT-TTF)$_2$Cu(NCS)$_2$ lifts up the degeneracy of the Landau levels converting them into the Landau bands. The width of the Landau bands and their positions oscillate in the changing magnetic field with the frequency of the closed α orbit producing MB satellite peaks in the FFT of the dHvA oscillations. Two satellites are most pronounced in the FFT at the frequencies $F_\beta - F_\alpha$ and $F_\beta + F_\alpha$ around the central peak at F_β which is due to the MB-composed large β orbit.[11] Here we will show that taking account of the chemical potential oscillations improves the agreement between theory and experiment. In particular, the forbidden peak at $F_\beta - F_\alpha$ becomes larger in amplitude than the satellite at $F_\beta + F_\alpha$ only if both, the chemical potential oscillations and the MB, are taken into account. The term "forbidden" is used in the literature to stress that the appropriate classical trajectory is impossible since it requires a sudden reversal of the electron movement on parts of the trajectory in an external magnetic field. More details and the references on the problem of the forbidden frequencies in layered organic conductors are given in Ref. 11.

The paper is organized as follows. In Sec. II we develop a theory of the chemical potential oscillations in layered conductors with arbitrary dispersion within the layers. We apply this theory in Sec. III to the calculations of the magnetization oscillations in layered conductors with coherent magnetic-breakdown Landau bands within the planes. The numerical analysis of the FFT peak content for different combinations of the MB regimes with and without chemical potential oscillations as well as the comparison with the experimental FFT spectrum of the dHvA oscillations in ET salt κ-(ET)$_2$Cu(NCS)$_2$ are given in Sec. IV. The main results and conclusions are summarized in Sec. V.

II. CHEMICAL POTENTIAL OSCILLATIONS IN LAYERED CONDUCTOR WITH ARBITRARY DISPERSION WITHIN THE LAYERS

We consider first the chemical potential oscillations in layered conductor with a closed 2D Fermi surface of arbitrary shape and arbitrary dispersion across the layers. Our final goal is to calculate the dHvA oscillations in ET salts taking into account both MB and chemical potential oscillations. The coherent MB as well as the electron hopping across the layers in layered conductors in an external magnetic field change the Lifshitz-Onsager quantization rules which can be written in the following general form:[11,22]

$$S(\varepsilon) = \frac{2\pi e\hbar B}{c}(n+\gamma) + 2\pi m_e \xi. \tag{1}$$

The parameter γ determines the Landau-band center position and ξ is the energy of the additional degrees of freedom related to the MB bands, interlayer hopping, and some other (such as spin, for example). We will assume in what follows that the variable ξ is distributed with the density of states (DOS) $g(\xi)$.

In this section, we generalize the results obtained in our recent paper[10] for the chemical potential quantum magnetic oscillations in layered 2D electron gas to the case of an arbitrary dispersion within the layers. Then we apply them to the dHvA calculation for Q2D metals with magnetic breakdown, such as ET salts. The total DOS for the system in question is

$$\rho(\varepsilon,B) = s\int_{-\infty}^{\infty} d\xi g(\xi) \sum_{n=0}^{\infty} \delta(\varepsilon - \varepsilon_{n\xi}), \tag{2}$$

where $\varepsilon_{n\xi}$ is a solution to Eq. (1), $s = \Phi/\Phi_0$ is the Landau levels degeneracy, and Φ_0 stands for the flux quantum.

To calculate the sum in Eq. (2) we have to use the Poisson summation rule applied to an arbitrary function of the type $f(n+\gamma)$, which yields

$$\sum_{n=0}^{\infty} f(n+\gamma) = \int_0^{\infty} f(x)dx + 2\mathrm{Re}\sum_{p=1}^{\infty} e^{-2\pi i p\gamma}\int_0^{\infty} f(x)e^{2\pi i p x}dx. \tag{3}$$

With the help of this summation rule, the DOS in Eq. (2) can be presented as a sum of a smooth $[\rho_0(\varepsilon,B)]$ and oscillating $[\tilde{\rho}(\varepsilon,B)]$ part

$$\rho(\varepsilon,B) = \rho_0(\varepsilon,B) + \tilde{\rho}(\varepsilon,B). \tag{4}$$

Explicitly, the terms in the right-hand side Eq. (4) can be written as follows:

$$\rho_0(\varepsilon,B) = s\frac{\eta}{\hbar\omega_c}\int_{-\infty}^{S(\varepsilon)/2\pi m_e} d\xi g(\xi), \tag{5}$$

$$\tilde{\rho}(\varepsilon,B) = \frac{s\eta}{\hbar\omega_c}\mathrm{Re}\sum_{p=1}^{\infty} \exp\{2\pi i p[S(\varepsilon)\Lambda^{-1} - \gamma]\}R_D(p)I_p. \tag{6}$$

Here, $\omega_c = eB/cm_e$ is the cyclotron frequency of free electrons. The effective mass of electron is determined by the standard equation $m^* = 1/2\pi[\partial S(\varepsilon)/\partial\varepsilon]$ and the exponential Dingle factor $R_D(p) = \exp(-pa\eta T_D/B)$ describes the Lorentz-like broadening of the Landau levels due to impurities in terms of the Dingle temperature T_D. Other notations are: $\eta = m^*/m_e$, $a = 2\pi^2 m_e k_B/e\hbar = 14.69TK^{-1}$, $\Lambda = 2\pi e\hbar B/c$, and the factor I_p is given by

$$I_p = \int_{-\infty}^{\infty} d\xi g(\xi) \exp\left(-\frac{2\pi i p \xi}{\hbar\omega_c}\right). \qquad (7)$$

Having at hand Eqs. (4), (5), and (6) for the DOS we can calculate the thermodynamic potential as a sum of the oscillating and steady parts

$$\Omega(\mu,B,T) = \Omega_0(\mu,B,T) + \tilde{\Omega}(\mu,B,T), \qquad (8)$$

where

$$\Omega(\mu,B,T) = -T\int_0^{\infty} \rho(\varepsilon,B) \ln\left[1 + \exp\left(\frac{\mu-\varepsilon}{T}\right)\right] d\varepsilon. \qquad (9)$$

The chemical potential as a function of magnetic field, $\mu(B)$, satisfies the equation $N=(\partial\Omega/\partial\mu)_{T,B}$, where the total number of the electrons in the system, N, is assumed to be fixed and related to the Fermi energy ε_F by the equation

$$N = \int_0^{\infty} \frac{\rho_0(\varepsilon, B=0)}{1 + \exp\left(\frac{\varepsilon-\varepsilon_F}{T}\right)} d\varepsilon. \qquad (10)$$

This equation is nothing but a definition of the Fermi energy in the system without external magnetic field. Repeating then the calculation steps of our paper[10] which for the problem in question are basically the same, we obtain

$$\tilde{\Omega} = \frac{s\hbar\omega_c}{2\pi^2\eta} \mathrm{Re} \sum_{p=1}^{\infty} \frac{1}{p^2} \exp\left[2\pi i p\left(S(\mu)\Lambda^{-1} - \gamma\right)\right] \times R_D(p) R_T(p) I_p. \qquad (11)$$

The temperature factor is given by

$$R_T(p) = \frac{\lambda p}{\sinh(\lambda p)}, \qquad (12)$$

with parameter $\lambda \equiv 2\pi^2 T\eta/\hbar\omega_c$. The oscillating part of the chemical potential $\tilde{\mu}=\mu-\varepsilon_F \ll \varepsilon_F$ then is easy to write in the following form:

$$\tilde{\mu} = \frac{\hbar\omega_c}{\eta D(\varepsilon_F)} \mathrm{Im} \sum_{p=1}^{\infty} \frac{1}{\pi p} \exp\left[2\pi i p\left(\frac{S(\varepsilon_F) + 2\pi m^* \tilde{\mu}}{\Lambda} - \gamma\right)\right] \times R_D(p) R_T(p) I_p. \qquad (13)$$

The factor $D(\varepsilon_F)$ renormalizing the chemical potential oscillation amplitude is determined by

$$D(\varepsilon_F) = \int_{-\infty}^{S(\varepsilon_F)/2\pi m_e} d\xi g(\xi). \qquad (14)$$

The corresponding equation for the oscillating part of the magnetization $\tilde{M} = -(\partial\tilde{\Omega}/\partial B)|_{\mu,N}$ in an explicit form reads

$$\tilde{M}(B) = \frac{eA}{2\pi^2\hbar c} \frac{S(\mu)}{m^*} \mathrm{Im} \sum_{p=1}^{\infty} \frac{1}{p} \times \exp\left[2\pi i p\left(\frac{S(\mu) + 2\pi m^* \tilde{\mu}}{\Lambda} - \gamma\right)\right] R_D(p) R_T(p) I_p. \qquad (15)$$

Here A is the area of the sample (conducting layer). The area inside the closed 2D Fermi surface in view of the inequalities $\hbar\omega_c, \tilde{\mu}(B) \ll \varepsilon_F$ can be approximated as $S(\mu) \approx S(\varepsilon_F)$.

Equations (13), (14), and (15) generalize the results obtained in Ref. 10 for the layered electron gas to the case of layered conductors with arbitrary electronic dispersion within the layers. In the next section we will apply these results to the organic ET salts which, similar to κ-$(\mathrm{ET})_2\mathrm{Cu(NCS)}_2$, display the magnetic breakdown behavior in dHvA experiments.

III. DHVA AND CHEMICAL POTENTIAL OSCILLATIONS IN MAGNETIC BREAKDOWN LAYERED CONDUCTOR

Consider now an application of the equations obtained in the preceding section to the case of the organic conductor κ-$(\mathrm{BEDT\text{-}TTF})_2\mathrm{Cu(NCS)}_2$. The dHvA oscillations in this layered compound have been considered in detail in Ref. 11 under the assumption that the chemical potential does not oscillate as a function of applied perpendicular magnetic field B. It was shown that the calculated oscillation pattern, as well as the FFT spectrum, basically correspond to the experimental observations. The principal idea of these calculations was that the coherent magnetic breakdown between the open sheets of the 2D Fermi surface and the closed orbits lifts up the Landau levels degeneracy and produces the Landau bands. The Landau bandwidth and position oscillations in the changing magnetic field, in particular, explain the appearance of the forbidden frequencies in the FFT. The β peak in the FFT spectrum has two nearby satellites $\beta-\alpha$ and $\beta+\alpha$. We will show in what follows that, in complete correspondence with the experiment, the intensity of the "forbidden" peak $\beta-\alpha$ is higher than that of the satellite peak $\beta+\alpha$ if we take into account oscillations of the chemical potential. For a fixed value of the chemical potential the intensities of the satellites are approximately equal.

The energy spectrum for κ-$(\mathrm{BEDT\text{-}TTF})_2\mathrm{Cu(NCS)}_2$ in a quantizing magnetic field perpendicular to the layers was calculated in detail in our previous paper.[11] Here, we only briefly discuss the basic results necessary for further consideration.

At low magnetic fields, the electrons within the layers move along the two open sheets of the Fermi surface and around the closed orbits situated between these sheets. Only the closed α orbits are quantized in that limit and the FFT of the magnetization oscillation pattern contains only the fundamental α peak and its harmonics, if the temperature and electron scattering (or the Dingle temperature T_D) are not too high. When B exceeds the magnetic breakdown field B_0 the tunneling between the open sheets and closed orbits becomes essential. Its probability is given by the square of the MB amplitude

$$\rho = \exp\left(-\frac{B_0}{2B}\right). \tag{16}$$

The conjugate quantum amplitude for the continuation of the motion along the same section of the Fermi surface without tunneling at the MB center is τ. The normalization condition for these amplitudes is $|\rho|^2+|\tau|^2=1$.

The MB center is the point where the two classical trajectories from the neighboring Brillouin zones are the closest. In the vicinity of the MB center electrons can tunnel from one trajectory to another composing a new trajectory. In ET salts, therefore, the magnetic breakdown makes possible electron motion around yet another closed trajectory, the β orbit. This orbit is composed of the two sections of the open sheets and the two sections of the α orbits between them connected into a closed trajectory by the MB centers. The quantization rules for the α and β orbits relating the energy ε with the quantum number n and quasi-wave-vector q, describing the electron dispersion within the Landau bands, are given by[11]

$$S_\alpha = \frac{2\pi eB\hbar}{c}\left[(n+1/2) + \frac{(-1)^n}{\pi}\arcsin(|\tilde{\rho}_{\text{eff}}|\cos qL)\right], \tag{17}$$

$$S_\beta = \frac{2\pi eB\hbar}{c}\left[(n+\gamma_{\text{eff}}) + \frac{(-1)^n}{\pi}\arcsin(|\tau_{\text{eff}}|\cos qL)\right]. \tag{18}$$

Here $S_\alpha(\varepsilon)$ and $S_\beta(\varepsilon)$ are the cross section areas enclosed by the α and β orbits in the momentum space and $\tilde{\rho}_{\text{eff}}$ and τ_{eff} are the effective MB amplitudes. The $|\tilde{\rho}_{\text{eff}}|=\rho^2$ is the effective amplitude for the electron hopping between the neighboring α orbits. The amplitude τ_{eff} is responsible for the resonant MB tunneling between the β orbits. It is given by equation[11] $|\tau_{\text{eff}}|=(1-|\rho_{\text{eff}}|^2)^{1/2}$. The effective probability of the MB through the closed α orbit equals to

$$|\rho_{\text{eff}}|^2 = \frac{\rho^4}{\rho^4+4(1-\rho^2)\sin^2\varphi_\alpha}. \tag{19}$$

This quantity oscillates in the inverse magnetic field with the frequency of the closed orbit $\varphi_\alpha=(\pi F_\alpha/B)$ which is proportional to the cross section area of the α orbit in momentum space at the Fermi level $S_\alpha(\varepsilon_F)$:

$$F_\alpha = \frac{cS_\alpha(\varepsilon_F)}{2\pi e\hbar}. \tag{20}$$

The parameter γ_{eff} in Eq. (18) is also an oscillating function of φ_α:

$$\gamma_{\text{eff}} = -\frac{1}{\pi}\left[\arctan\left(\frac{1+\tau^2}{1-\tau^2}\tan\varphi_\alpha\right)-\varphi_\alpha\right]. \tag{21}$$

The quantization rules for the quantities $S_\alpha(\varepsilon)$ and $S_\beta(\varepsilon)$ in Eqs. (17) and (18) can be written in the form of Eq. (1). To do this note that the dispersion relations of electrons within the α and β Landau bands are given by the equations

$$\varepsilon_{\alpha(\beta)}(q) = \frac{\hbar\omega_c}{\eta_{\alpha(\beta)}\pi}\arcsin(W_{\alpha(\beta)}\cos qL), \tag{22}$$

where $W_\alpha=\rho^2$, $W_\beta=(1-|\rho_{\text{eff}}|^2)^{1/2}$, and $\eta_{\alpha(\beta)}=m^*_{\alpha(\beta)}/m_e$. The dispersion relation (22) means that Eqs. (17) and (18) are of the same form as Eq. (1) since the corresponding densities of state within the Landau bands $g_{\alpha(\beta)}(\varepsilon)$ can be easily calculated. This allows an easy generalization of the results obtained in the preceding section for one band to the case of two bands with arbitrary dispersion. In this case the total DOS is a sum of the two terms

$$\rho(\varepsilon,B) = \rho_\alpha(\varepsilon,B)+\rho_\beta(\varepsilon,B). \tag{23}$$

The corresponding thermodynamic potential is a sum of the steady part and two oscillating terms

$$\Omega(\mu,B,T) = \Omega_0(\mu,B,T)+\tilde{\Omega}_\alpha(\mu,B,T)+\tilde{\Omega}_\beta(\mu,B,T). \tag{24}$$

The explicit equations for the oscillating contributions to the thermodynamic potential are given by

$$\tilde{\Omega}_{\alpha(\beta)} = \text{Re}\sum_{p=1}^{\infty}\frac{1}{p^2}\exp\left[2\pi ip\left(\frac{cS_{\alpha(\beta)}(\mu)}{2\pi e\hbar B}-\gamma_{\alpha(\beta)}\right)\right] \times \frac{s\hbar\omega_c}{2\pi^2\eta_{\alpha(\beta)}}R_D^{\alpha(\beta)}(p)R_T^{\alpha(\beta)}(p)R_S^{\alpha(\beta)}(p)I_p^{\alpha(\beta)}. \tag{25}$$

Here, $\gamma_\alpha=1/2$ for the α orbit and $\gamma_\beta=\gamma_{\text{eff}}$ for the β orbit. In what follows all the quantities of the previous section acquire band indices. For example, $S(\varepsilon)\to S_{\alpha(\beta)}(\varepsilon)$, $m^*\to m^*_{\alpha(\beta)}$. Correspondingly, the temperature and Dingle factors become

$$R_T^{\alpha(\beta)} = \frac{\lambda_{\alpha(\beta)}p}{\sinh(\lambda_{\alpha(\beta)}p)}, \quad R_D^{\alpha(\beta)} = \exp\left(-\frac{pa\eta_{\alpha(\beta)}T_D^{\alpha(\beta)}}{B}\right). \tag{26}$$

We introduced also the spin factor for the sake of completeness

$$R_S^{\alpha(\beta)} = \cos\left[\frac{\pi}{2}pg_{\alpha(\beta)}\eta_{\alpha(\beta)}\right]. \tag{27}$$

The notation $g_{\alpha(\beta)}$ represents the g factor for the α and β orbit. The Landau band factors, $I_p^{\alpha(\beta)}(W_{\alpha(\beta)})$, appear due to the dispersion relations within the Landau bands in Eq. (22). These factors are a generalisation of Eq. (7) to the α and β Landau bands, which yields

$$I_p^{\alpha(\beta)}(W_{\alpha(\beta)}) = \frac{2}{\pi}\int_0^{\pi/2}dy\,\cos\left[2p\arcsin(W_{\alpha(\beta)}\cos y)\right]. \tag{28}$$

Taking a derivative of the thermodynamic potential with respect to the magnetic field, we have for the magnetization $\tilde{M}(B)$:

$$\tilde{M}(B) = \tilde{M}_\alpha(B) + \tilde{M}_\beta(B), \tag{29}$$

where

$$\tilde{M}_\alpha(B) = M_\alpha^0 \sum_{p=1}^{\infty} \frac{(-1)^{(p+1)}}{p} \sin\left[2\pi p\left(\frac{F_\alpha}{B} + \eta_\alpha \frac{\tilde{\mu}}{\hbar\omega_c}\right)\right] \times I_p^\alpha(\rho^2) R_T^\alpha(p) R_S^\alpha(p) R_D^\alpha(p), \tag{30}$$

$$\tilde{M}_\beta(B) = M_\beta^0 \sum_{p=1}^{\infty} \frac{1}{p} \sin\left[2\pi p\left(\frac{F_\beta}{B} + \eta_\beta \frac{\tilde{\mu}}{\hbar\omega_c} - \gamma_{\text{eff}}\right)\right] \times I_p^\beta(|\tau_{\text{eff}}|) R_T^\beta(p) R_S^\beta(p) R_D^\beta(p). \tag{31}$$

The prefactors in these equations are defined as

$$M_{\alpha(\beta)}^0 = \frac{eA}{2\pi^2\hbar c} \frac{S_{\alpha(\beta)}(\varepsilon_F)}{m_{\alpha(\beta)}^*}. \tag{32}$$

The oscillation frequencies are proportional to the area enclosed by the α and β orbits in the momentum space $F_{\alpha(\beta)} = cS_{\alpha(\beta)}(\varepsilon_F)/2\pi e\hbar$.

The equation for the chemical potential is given by

$$\mu = \varepsilon_F + \tilde{\mu} \text{ and } \tilde{\mu} = \frac{\hbar\omega_c}{D_{\text{eff}}(\varepsilon_F)}(\tilde{\mu}_\alpha + \tilde{\mu}_\beta), \tag{33}$$

where

$$\tilde{\mu}_\alpha = \sum_{p=1}^{\infty} \frac{(-1)^{(p+1)}}{\pi p} \sin\left[2\pi p\left(\frac{F_\alpha}{B} + \eta_\alpha \frac{\tilde{\mu}}{\hbar\omega_c}\right)\right] \times I_p^\alpha(\rho^2) R_T^\alpha(p) R_S^\alpha(p) R_D^\alpha(p), \tag{34}$$

$$\tilde{\mu}_\beta = \sum_{p=1}^{\infty} \frac{1}{\pi p} \sin\left[2\pi p\left(\frac{F_\beta}{B} + \eta_\beta \frac{\tilde{\mu}}{\hbar\omega_c} - \gamma_{\text{eff}}\right)\right] \times I_p^\beta(|\tau_{\text{eff}}|) R_T^\beta(p) R_S^\beta(p) R_D^\beta(p). \tag{35}$$

The factor $D_{\text{eff}}(\varepsilon_F)$, decreasing the amplitude of the chemical potential oscillations in Eq. (33), is a generalization of the corresponding factor obtained in Ref. 10 to the case of the ET salts with the more complex two-band Fermi surface. It is given by the sum

$$D_{\text{eff}}(\varepsilon_F) = \eta_\alpha D_\alpha(\varepsilon_F) + \eta_\beta D_\beta(\varepsilon_F), \tag{36}$$

where

$$D_{\alpha(\beta)}(\varepsilon_F) = \int_{-\infty}^{S_{\alpha(\beta)}(\varepsilon_F)/2\pi m_e} d\xi g_{\alpha(\beta)}(\xi). \tag{37}$$

The Landau band factor $I_p^{\alpha(\beta)}(W_{\alpha(\beta)})$ standing in the equations for the magnetization and chemical potential can be written in an explicit form as

$$I_p^{\alpha(\beta)}(W_{\alpha(\beta)}) = 1 + \sum_{k=1}^{p} \frac{(-1)^k}{(k!)^2} W_{\alpha(\beta)}^{2k} \prod_{l=0}^{k-1} (p^2 - l^2). \tag{38}$$

This factor, as a function of the $0 \leqslant W_{\alpha(\beta)} \leqslant 1$, is a polynomial with fixed values at the boundaries $I_p^{\alpha(\beta)}(0) = 1$ and $I_p^{\alpha(\beta)}(1) = 0$. For the first three indices $p = 0, 1, 2, \ldots$, we have

$$I_0^{\alpha(\beta)} = 1, \quad I_1^{\alpha(\beta)} = 1 - W_{\alpha(\beta)}^2, \quad I_2^{\alpha(\beta)} = 1 - 4W_{\alpha(\beta)}^2 + 3W_{\alpha(\beta)}^4. \tag{39}$$

Note that because $W_\beta = (1 - |\rho_{\text{eff}}|^2)^{1/2}$ is a strongly oscillating function of the inverse magnetic field, due to the term $\sin^2(\pi F_\alpha/B)$ in Eq. (19), the factor $I_p^\beta(W_\beta)$ oscillates in rather nontrivial fashion too. For example, the oscillations of $\tilde{M}(B)_\beta$ are determined by the factor $I_p^\beta(|\tau_{\text{eff}}|)$ which for the first harmonic yields $I_1^\beta(|\tau_{\text{eff}}|) = 1 - |\tau_{\text{eff}}|^2 = |\rho_{\text{eff}}|^2 \propto \exp(-B_0/B)$. Therefore, we see that because of the MB the contribution of the β orbit to the total magnetization oscillation pattern grows with magnetic field and oscillates with the frequency of the closed α orbit. These orbits play the role of the effective resonant MB centers between the β orbits due to the interference of the quantum amplitudes corresponding to the multiple closed pathways around them (the so called Stark interferometer). In real samples these amplitudes are damped which means that a nonzero imaginary part has to be added to the phases in Eq. (19): $\varphi_\alpha \to \varphi_\alpha - i\Gamma(B)/2$. Physically this is because of the small-angle scattering caused by phonons, dislocations and other types of the smooth random potential which does not affect oscillations through the Dingle factor, but cause the decoherence destroying the MB interference.[23] In particular, the effective amplitude $|\tau_{\text{eff}}|$with respect of the above decoherence parameter Γ becomes

$$|\tau_{\text{eff}}| = \tau\left(\frac{(1 + e^{-\Gamma})^2 - 4e^{-\Gamma}\cos^2\varphi_\alpha}{(1 + \tau^2 e^{-\Gamma})^2 - 4\tau^2 e^{-\Gamma}\cos^2\varphi_\alpha}\right)^{1/2}. \tag{40}$$

The limit $\Gamma(B) \gg 1$ corresponds to the incoherent (stochastic) magnetic breakdown regime when the oscillations due to the phase $\varphi_\alpha = 2\pi F_\alpha/B$ are suppressed.[23] Nonetheless, it follows from Eq. (40) that for small values of ρ, when τ is of the order unity, the quantity $|\tau_{\text{eff}}|$ oscillates with the amplitude of the order of τ if $\Gamma < 1$. On the other hand, incoherence strongly suppresses the oscillations in $|\gamma_{\text{eff}}|$ as one can see from Eq. (21) after the substitution $\varphi_\alpha \to \varphi_\alpha - i\Gamma(B)/2$. For example, a substitution $|\tan(\varphi_\alpha)| \to |\tan(\varphi_\alpha - i\Gamma/2)|$ supresses the singularities of the function $\tan(\varphi_\alpha)$ and decreases the amplitude with the increase of the incoherence factor Γ. A numerical analysis shows that, for any set of parameters relevant to the experiment in question, variations in the amplitude of $|\gamma_{\text{eff}}|$ are approximately two orders of magnitude less than that of $|\tau_{\text{eff}}|$. In particular, for $\tau = 0.9$ the oscillation amplitudes of $|\tau_{\text{eff}}|$ decrease gradually from 0.9 to 0.2 when Γ is varied from 0.01 to 1, while the amplitudes of $|\gamma_{\text{eff}}|$ decrease gradually from 0.0003 to 0.0001. At $\Gamma = 0$ a pure coherent case recovers.

As was shown in Ref. 11 the organic salt κ-(BEDT$-$TTF)$_2$Cu(NCS)$_2$ is most likely in a weakly incoherent regime $\Gamma \sim 1$. In general, the problem of the decoherence due to the small-angular scattering in the periodic magnetic breakdown systems is very complex. We use in the next section the simple phenomenology of the paper[23] to incorporate this effect in terms of Γ into numerical calculations for the organic salt κ-(BEDT$-$TTF)$_2$Cu(NCS)$_2$.

IV. THE RESULTS OF THE NUMERICAL ANALYSIS AND COMPARISON WITH EXPERIMENT

The equations for the magnetization and the chemical potential oscillations obtained in the preceding section are complex and can be analyzed only numerically. The numerical analysis of the dHvA experimental data in the organic ET salt κ-(BEDT−TTF)$_2$Cu(NCS)$_2$ was done in our previous publication under the assumption that the chemical potential does not vary as a function of magnetic field. Here, we will show that taking account of the chemical potential oscillations makes the fit with the experiment better. The fit is the best if we use the following parameters. The effective masses, frequencies, the MB field B_0, and g factors are known from the literature[11] $m_\alpha=3.55m_e$, $m_\beta=7m_e$, $F_\alpha=639.5$ T, $F_\beta=4166$ T, $g_\alpha=1.6$, $g_\beta=1.52$. The magnetic breakdown field in κ -(BEDT−TTF)$_2$Cu(NCS)$_2$is $B_0=30$ T. The Dingle temperatures and the decoherence factor are the fitting parameters which we take as follows: $T_D^\alpha=0.36$ K, $T_D^\beta=0.29$ K, $\Gamma(B)=\Gamma_0 B$, where $\Gamma_0=0.085$ T^{-1}. The temperature of the experiment is $T=0.395$ K and the field interval is $(20-27)$ T.

T_D^α is determined from the low-field part of the Dingle plot[11,14]. In that field region $(B \ll B_0)$ contributions from the magnetic-breakdown β orbit and satellites $\beta\pm\alpha$ are negligible. (The value $T_D^\alpha=0.6$K in Ref. 11 is a misprint. The correct value is $T_D^\alpha=0.36$ K.) The direct determination of T_D^β within the LK approach is not feasible since it is impossible to extract from the experimental data that part of the field-dependent β amplitude which is due to the scattering effect by disorder. In our approach amplitudes of the magnetic-breakdown peaks (β orbit and satellites $\beta\pm\alpha$) in the FFT spectrum are controlled by the two parameters T_D^β and Γ_0. Their choice is more or less unique when a fit to the experimental FFT peaks of these orbits is made. After the MB field is fixed, T_D^β controls the β peak amplitude and the heights of the satellites depends on Γ_0. The results of the numerical analysis are summarized in Figs. 1–4 and Table I. The fit to the experimental magnetization oscillations in κ-(BEDT−TTF)$_2$Cu(NCS)$_2$ is better than in Ref. 11. The difference between the theoretical and experimental magnetization curves can be hardly resolved by naked eye. In view of that it is more informative to analyse the fast Fourier transform graphs. The theoretical FFT spectrum for κ-(BEDT−TT)$_2$Cu(NCS)$_2$ at $T=0.395$ K and for the above choice of parameters is shown in Fig. 1. The typical feature of this picture is the presence of the peaks at frequencies F_α, $2F_\alpha$, F_β, and two distinct satellites around the latter peak. The left satellite, $\beta-\alpha$, is "forbidden" and higher than the right satellite, $\beta+\alpha$. The experimental FFT graph (see Ref. 11) has exactly the same peculiarities. To clear up which of the factors is responsible for these peculiarities we plot the FFT graphs shown in Figs. 2 and 3. In Fig. 2 we take $\mu=$const and suppress the oscillations in τ and ρ, by $\Gamma \gg 1$, which implies the stochastic MB regime. We see that the satellites around the β peak are suppressed too in that case. The result for the coherent MB regime with fixed value of the chemical potential is shown in Fig. 3. Here, we take into account oscillations of τ and ρ replacing them by the effective quantities. We see that the satellites in Fig. 3 have nonzero and equal amplitudes. The corresponding figure for the FFT spectrum in our previous work[11] has more satellites around the β peak because we did not take into account the suppression of the oscillations in γ_{eff} due to the decoherence. One can see from Figs. 1–3 and Table I that the amplitudes of the α and β peaks remain approximately constant for all three regimes, but the amplitudes of the 2α peak and satellites at the frequencies $F_\beta \pm F_\alpha$ do change. To see these changes in more detail we present their amplitudes in Table I and plot these peaks in an enlarged scale in Fig. 4. The peak at the frequency $2F_\alpha$ is seen to be the highest for a fixed value of the chemical potential (Figs. 2 and 3) both in the stochastic and coherent MB regimes. In the stochastic regime the satellites $\beta\pm\alpha$ are suppressed (Fig. 2), but in the coherent MB regime (Fig. 3) the peaks at the frequencies $F_\beta \pm F_\alpha$ become much larger. The peak at the frequency $2F_\alpha$ decreases when chemical potential oscillations are taken into account (Fig. 1). The satellites $\beta\pm\alpha$ are enhanced and the amplitude of the forbidden satellite $\beta-\alpha$ becomes larger than the peak at the frequency $F_\beta+F_\alpha$, as is clearly seen in Fig. 4. The numerical values for all these amplitudes given in Table I are in a good agreement with the experiment.

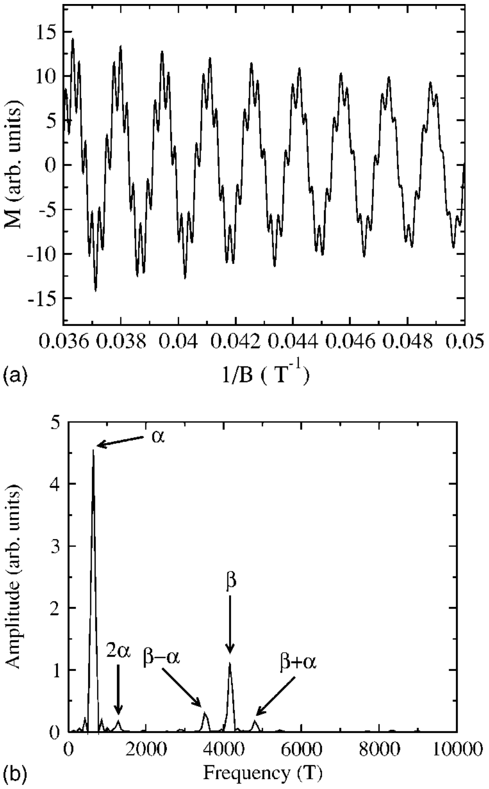

FIG. 1. The calculated magnetization oscillation pattern M(B) (upper picture) and its FFT (lower picture) in the coherent MB regime with taking account of the chemical potential oscillations. The peaks in the FFT spectrum correspond to the closed α-orbit (α and 2α) and those, which are due to the magnetic breakdown (β and satellites $\beta\pm\alpha$). The satellite $\beta-\alpha$ corresponds to the so-called "forbidden trajectory" at the Fermi surface (see text for details).

The above numerical analysis permits us to conclude that only if we take into account oscillations of the chemical

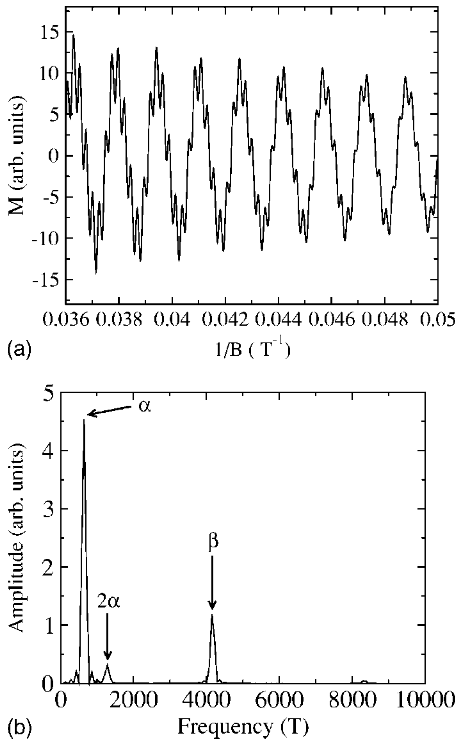

FIG. 2. The magnetization oscillation pattern (upper picture) and its FFT (lower picture) in the case of a fixed chemical potential in the stochastic MB regime. Notations for the peaks in the FFT are the same as in Fig. 1.

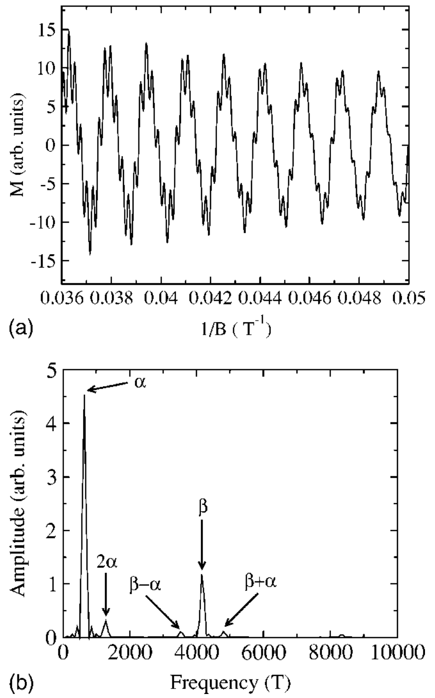

FIG. 3. The magnetization oscillation pattern (upper picture) and its FFT (lower picture) in the case of a fixed chemical potential in the coherent MB regime. Notations for the peaks in the FFT are the same as in Fig. 1.

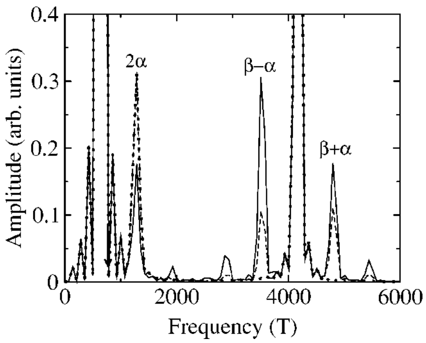

FIG. 4. The small FFT-peaks from Figs. 1–3 on a large scale: (i) (solid line) the coherent MB regime with the chemical potential oscillations (Fig. 1). Note that the higher harmonics 3α and MB satellites $\beta \pm 2\alpha$ are resolved in this graph. (ii) (dotted line) the case of the fixed chemical potential in the stochastic MB regime (Fig. 2). (iii) (dashed line) the case of the fixed chemical potential in the coherent MB regime (Fig. 3).

potential and the MB-driven oscillations of the Landau-band spectrum, we obtain a correct FFT shown in Fig. 1. In this picture, in full agreement with the experiment, the amplitude of the forbidden satellite $\beta-\alpha$ is larger than that of $\beta+\alpha$. The magnetization-oscillation patterns in Figs. 1–3 look very much the same for the naked eye but the corresponding FFT graphs display a clear-cut distinction between them. In that sense the FFT spectrum is more informative than the magnetization oscillations. In particular, even a third harmonic at 3α and higher MB satellites at $\beta \pm 2\alpha$ are resolved in the FFT of Fig. 4 (solid line), i.e., in the coherent MB regime with chemical potential oscillation.

V. CONCLUSION

This paper is a continuation of our previous work[11] on the dHvA effect in Q2D organic metals with MB, such as ET salt κ-(BEDT−TTF)$_2$Cu(NCS)$_2$. In Ref. 11 we have shown that the so-called forbidden frequencies in the FFT spectrum of the quantum magnetic oscillations is a consequence of the Landau quantization under the condition of coherent magnetic breakdown. Both the Landau bandwidth and their positions oscillate in the magnetic field with the frequency of the α orbit F_α. These oscillations explain the appearance of the forbidden frequencies such as $F_\beta - F_\alpha$ in the FFT of the magnetization which in the coupled-network model of the

TABLE I. Comparison between the experimental and calculated values of the magnetic breakdown amplitudes and the second harmonics $2F_\alpha$. All values are given in units of the highest FFT α-peak amplitude.

	$2F_\alpha$	$F_\beta - F_\alpha$	F_β	$F_\beta + F_\alpha$
Experiment	0.051	0.093	0.263	0.051
Fig. 1	0.046	0.078	0.249	0.046
Fig. 2	0.079	~0	0.259	~0
Fig. 3	0.079	0.032	0.259	0.032

MB should be prescribed to the reversed sense of electron rotation at some sections of the 2D Fermi surface.

In this paper, we take into account jointly the coherent MB effects and the chemical potential oscillations and gain a better agreement with the experimental FFT spectrum of the dHvA oscillations of κ-$(\mathrm{BEDT-TTF})_2\mathrm{Cu(NCS)}_2$ than in our previous work.[11] In Ref. 11 the chemical potential was assumed to be fixed. Here, we took account of the chemical potential oscillatons. We first developed in Sec. II a theory of the chemical potential oscillations in layered conductors with the arbitrary electron dispersion within the layers. This theory is a generalization of our result for the chemical potential oscillations in layered electron gas and superlattices in quantizing magnetic field[10] to the case of arbitrary 2D dispersion. The numerical analysis and application of the results to the quasi 2D organic conductor κ-$(\mathrm{BEDT-TTF})_2\mathrm{Cu(NCS)}_2$ is summarized in Figs. 1–4 and Table I. It shows that the chemical potential oscillations in the coherent and stochastic MB regimes do not affect the α and β peaks, but change the amplitudes of the higher harmonics and the MB-driven satellites around the β peak. In the stochastic MB regime all satellites are depressed. In the coherent MB regime they grow higher and have equal amplitudes. We find that in the coherent MB regime with the chemical potential oscillations the agreement with the experiment is the best. The "forbidden" peak $\beta-\alpha$ in that case becomes higher than the right satellite $\beta+\alpha$. This is nontrivial, since the term "forbidden" means that the peak with the frequency $F_\beta - F_\alpha$ should not exist in the FFT spectrum at all according to the quasiclassical theories.

We believe that the results obtained in the present work will be useful for further researches of the quantum magnetic oscillations in layered conductors with magnetic breakdown. The calculations of the SdH conductivity for layered conductors with magnetic breakdown will be published elsewere.

ACKNOWLEDGMENTS

The authors acknowledge useful discussions with A.M. Dyugaev, P.D. Grigoriev, T. Maniv, and J. Wosnitza for reading the manuscript. The work was supported in part by INTAS program, Project No. INTAS-01-0791 and the NATO Collaborative Linkage Grant No. 977292. V.M.G. is grateful to P. Fulde and S. Flach for the hospitality at MPIPKS in Dresden. D.A.P. was supported by NSF Grant No. DMR-9984002 and by the David & Lucille Packard Foundation.

---

*On leave from the Kharkov National University, 61077, Kharkov, Ukraine.

[1] I. M. Lifshitz and A. M. Kosevich, Zh. Eksp. Teor. Fiz. **29**, 730 (1956) [Sov. Phys. JETP **2**, 636 (1956)].
[2] D. Shoenberg, *Magnetic Oscillations in Metals* (Cambridge University Press, Cambridge, 1984).
[3] A. A. Abrikosov, *Fundamentals of Theory of Metals* (North-Holland, Amsterdam, 1988).
[4] I. D. Vagner, T. Maniv, and E. Ehrenfreund, Phys. Rev. Lett. **51**, 1700 (1983); K. Jauregui, V. I. Marchenko, and I. D. Vagner, Phys. Rev. B **41**, 12 922 (1990); M. A. Itskovsky, T. Maniv, and I. D. Vagner, Z. Phys. B: Condens. Matter **101**, 13 (1996).
[5] M. Nakano, J. Phys. Soc. Jpn. **66**, 19 (1997).
[6] A. S. Alexandrov and A. M. Bratkovsky, Phys. Rev. Lett. **76**, 1308 (1986).
[7] P. D. Grigoriev and I. D. Vagner, Pis'ma Zh. Eksp. Teor. Fiz. **69**, 139 (1999) [JETP Lett. **29**, 156 (1999)].
[8] P. Grigoriev, Zh. Eksp. Teor. Fiz. **119**, 1257 (2001) [JETP **92**, 1090 (2001)].
[9] T. Champel, Phys. Rev. B **64**, 054407 (2001); T. Champel and V. P. Mineev, Philos. Mag. B **81**, 55 (2001).
[10] V. M. Gvozdikov, A. G. M. Jansen, D. I. Pesin, I. D. Vagner, and P. Wyder, Phys. Rev. B **68**, 155107 (2003).
[11] V. M. Gvozdikov, Yu. V. Pershin, E. Steep, A. G. M. Jansen, and P. Wyder, Phys. Rev. B **65**, 165102 (2002).
[12] F. A. Meyer, E. Steep, W. Biberacher, P. Christ, A. Lerf, A. G. M. Jansen, W. Joss, and P. Wyder, Europhys. Lett. **32**, 681 (1995).
[13] S. Uji, M. Chaparala, S. Hill, P. S. Sandhu, J. Qualls, L. Seger, and J. S. Brooks, Synth. Met. **85**, 1573 (1997).
[14] E. Steep, L. H. Nguyen, W. Biberacher, H. Muller, A. G. M. Jansen, and P. Wyder, Physica B **259-261**, 1079 (1999).
[15] C. P. Heidmann, H. Mueller, W. Biberacher, K. Neumaier, C. Probst, K. Andres, A. G. M. Jansen, and W. Joss, Synth. Met. **41-43**, 2029 (1991).
[16] T. Sasaki, H. Sato, and N. Toyota, Solid State Commun. **76**, 507 (1990).
[17] J. Caulfield, J. Singleton, F. L. Pratt, M. Doporto, W. Lubczynski, W. Hayes, M. Kurmoo, P. Day, P. T. J. Hendriks, and J. A. Perenboom, Synth. Met. **61**, 63 (1993).
[18] M. V. Kartsovnik, G. Yu. Logvenov, T. Ishiguro, W. Biberacher, H. Anzai, and N. D. Kushch, Phys. Rev. Lett. **77**, 2530 (1996).
[19] N. Harrison, J. Caulfield, J. Singleton, P. H. P. Reinders, F. Herlach, W. Hayes, M. Kurmoo, and P. Day, J. Phys.: Condens. Matter **8**, 5415 (1996).
[20] E. Steep, L. H. Nguyen, W. Biberacher, H. Muller, A. G. M. Jansen, and P. Wyder, Physica B **259-261**, 1079 (1999).
[21] J. Singleton, Rep. Prog. Phys. **63**, 1111 (2000).
[22] V. M. Gvozdikov, Fiz. Nizk. Temp. **12**, 705 (1986) [Sov. J. Low Temp. Phys. **12**, 399 (1986)].
[23] M. I. Kaganov and A. A. Slutskin, Phys. Rep. **98**, 189 (1983).